

The photo-disintegration of ${}^4\text{He}$ on the cosmic microwave background is less severe than earlier thought

Jorge F. Soriano,^{1,2} Luis A. Anchordoqui,^{1,2,3} and Diego F. Torres^{4,5,6}

¹*Department of Physics & Astronomy, Lehman College, City University of New York, NY 10468, USA*

²*Department of Physics, Graduate Center, City University of New York, NY 10016, USA*

³*Department of Astrophysics, American Museum of Natural History, NY 10024, USA*

⁴*Institute of Space Sciences (IEEC-CSIC), Campus UAB, Carrer de Magrans s/n, 08193 Barcelona, Spain*

⁵*Institució Catalana de Recerca i Estudis Avançats (ICREA), E-08010 Barcelona, Spain*

⁶*Institut d'Estudis Espacials de Catalunya (IEEC), 08034 Barcelona, Spain*

We thoroughly study the photo-disintegration of ${}^4\text{He}$ on the cosmic microwave background using the most recent cross-section data both from the inclusive measurement observing the analog of the giant dipole resonance in ${}^4\text{He}$ through the charge-exchange spin-flip ${}^4\text{He}({}^7\text{Li}, {}^7\text{Be})$ reaction and from measurements of exclusive two-body and three-body processes: ${}^4\text{He}(\gamma, p){}^3\text{H}$, ${}^4\text{He}(\gamma, n){}^3\text{He}$, and ${}^4\text{He}(\gamma, pn){}^2\text{H}$. We show that the present-day (redshift $z = 0$) mean free path of ultra-relativistic (Lorentz factor $\sim 10^{10}$) helium nuclei increases by more than 15% with respect to previous estimates adopted as benchmarks for Monte Carlo simulation codes of ultrahigh-energy cosmic ray propagation. This implies that the *physical* survival probability of ${}^4\text{He}$ nuclei would be larger than predicted by existing event generators. For example, for $E \sim 10^{10.8}$ GeV and a propagation distance of 3.5 Mpc, the ${}^4\text{He}$ intensity would be 35% larger than the output of CRPropa 3 program and 42% larger than the output of SimProp v2r4 program. We provide new parametrizations for the two-body and three-body photo-disintegration cross-sections of ${}^4\text{He}$, ${}^3\text{He}$, tritium, and deuterium.

I. INTRODUCTION

The Greisen-Zatsepin-Kuzmin (GZK) horizon of helium [1, 2] is a key parameter in ascertaining the contribution of ultrahigh-energy ($E \gtrsim 10^{10}$ GeV) cosmic rays (UHECRs) with directional pointing to nearby sources. Numerical [3, 4] and analytical [5] estimates of this parameter, as well as Monte Carlo simulation codes of UHECR propagation [6–11] are customarily based on fits [12–15] to cross-section measurements from the sixties [16–21], which do not allow a precise description of the giant dipole resonance (GDR) near threshold.

The first simultaneous measurement of the two-body and three-body photo-disintegration cross-sections of ${}^4\text{He}$ in the GDR region was carried out in 2005 at the National Institute of Advanced Industrial Science and Technology (AIST) [22]. Data from the three-body process yield a ${}^4\text{He}(\gamma, pn){}^2\text{H}$ cross section of 0.04 ± 0.01 mb at 29.8 MeV, in agreement with previous measurements [16–18, 23, 24]. However, the dominant ${}^4\text{He}(\gamma, p){}^3\text{H}$ and ${}^4\text{He}(\gamma, n){}^3\text{He}$ cross sections are found to increase monotonically with energy up to 29.8 MeV, in strong disagreement with previous observations [25–28]. Subsequently, a detailed study of the GDR in ${}^4\text{He}$ was carried out at the Research Center for Nuclear Physics (RCNP), using a 455 MeV ${}^7\text{Li}^{3+}$ beam bombarding a ${}^4\text{He}$ gas target cooled to about 10 K [29, 30]. An indirect measurement of the GDR in ${}^4\text{He}$ was obtained by observing its analog via the ${}^4\text{He}({}^7\text{Li}, {}^7\text{Be})$ reaction at forward scattering angles. The inclusive cross-section measurement from the ${}^4\text{He}({}^7\text{Li}, {}^7\text{Be})$ reaction also shows a radical departure from the results of the AIST group. Deepening the mystery, the ${}^4\text{He}$ photo-disintegration cross section was measured again by the same group at AIST, confirming their earlier findings [31]. To clarify the situa-

tion, the total (i.e. angle-integrated) cross-section of the exclusive two-body channels was measured at the High Intensity Gamma-ray Source (HIγS) [32, 33]. The HIγS experiment confirmed that the peak of the GDR is near 27 MeV and emphasized the differences with the AIST measurements. If we would assume that a systematic effect affected the AIST measurement of ${}^4\text{He}(\gamma, p){}^3\text{H}$ and ${}^4\text{He}(\gamma, n){}^3\text{He}$ and leave these aside, we may conclude that there is now a good agreement in the experimental front (see the data plotted in Fig. 1, top panel).

In this article we provide a new parametrization of the photo-disintegration cross-section of helium through a fit to the most recent data from the RCNP and HIγS experiments. Armed with this parametrization we re-examine the opacity of the cosmic microwave background (CMB) to ultra-relativistic (Lorentz factor $\sim 10^{10}$) helium nuclei.

II. NEW PARAMETRIZATION OF THE GDR IN ${}^4\text{He}$

The photo-absorption cross-section of a nucleus of charge Ze and baryon number A roughly obeys the Thomas-Reiche-Kuhn (TRK) dipole sum rule [34–36]

$$\Sigma = \int_0^\infty \sigma_A(\varepsilon) d\varepsilon = 59.8 \frac{Z(A-Z)}{A} \text{ MeV mb}. \quad (1)$$

Symmetric resonant cross-sections are commonly fitted by the normal distribution, with probability density function given by

$$f_{\mathcal{N}}(\mu, \Gamma; \varepsilon) \equiv \frac{1}{\sqrt{2\pi}\Gamma} \exp\left[-\frac{(\varepsilon - \mu)^2}{2\Gamma^2}\right], \quad (2)$$

where μ is the mean and Γ measures the dispersion around the mean.

The features of the cross-section data of the nuclei analyzed herein make evident that the GDR does not follow a symmetric curve around its central value. A simple way to account for the antisymmetry when the fall on the right side of the central value is much slower than the rise on the left side is to consider logarithmic distributions. These can be obtained as $g(x) dx = f(\ln x) d \ln x$, if f is a symmetric distribution, which gives $g(x) = f(\ln x)/x$ for $x > 0$. To accommodate threshold effects we can simply shift the independent variable so that the threshold is at some value x_{th} rather than 0.

To model the shape of the photo-disintegration cross-section in the energy range of the GDR we adopt the shifted log-normal distribution. Substituting ε for $\ln(\varepsilon - \varepsilon_{th})$ in (2) and introducing the $1/(\varepsilon - \varepsilon_{th})$ factor, we arrive at the cross-section density function

$$\sigma_A(\sigma_0, \varepsilon_0, \varepsilon_{th}, \Gamma; \varepsilon) = \sigma_0 \exp \left[-\frac{\ln^2 \left(\frac{\varepsilon - \varepsilon_{th}}{\varepsilon_0 - \varepsilon_{th}} \right)}{2\Gamma^2} \right], \quad (3)$$

where ε_0 is the central value of the GDR energy band (with threshold ε_{th}), σ_0 is the cross section at $\varepsilon = \varepsilon_0$, and Γ is a measurement of the dispersion around ε_0 .

For analytical order of magnitude estimates, it is convenient to obtain a form of the cross-section in the single pole of the narrow-width approximation (NWA). Introducing the change of variables

$$z(\varepsilon) \equiv \ln \left(\frac{\varepsilon - \varepsilon_{th}}{\varepsilon_0 - \varepsilon_{th}} \right) \quad (4)$$

we have

$$\sigma_A(\sigma_0, \varepsilon_0, \varepsilon_{th}, \Gamma; \varepsilon) \propto f_{\mathcal{N}}(0, \Gamma; z(\varepsilon)). \quad (5)$$

For the normal distribution,

$$\begin{aligned} \lim_{\Gamma \rightarrow 0} f_{\mathcal{N}}(0, \Gamma; z(\varepsilon)) &= \delta(z(\varepsilon)) = \frac{\delta(\varepsilon - \varepsilon_0)}{|z'(\varepsilon_0)|} \\ &= (\varepsilon_0 - \varepsilon_{th}) \delta(\varepsilon - \varepsilon_0), \end{aligned} \quad (6)$$

and so we can approximate (3) as

$$\sigma_A(\sigma_0, \varepsilon_0, \varepsilon_{th}, \Gamma; \varepsilon) \approx \mathcal{A} \delta(\varepsilon - \varepsilon_0), \quad (7)$$

where \mathcal{A} is the normalization constant satisfying

$$\int_{\varepsilon_{th}}^{\infty} \mathcal{A} \delta(\varepsilon - \varepsilon_0) d\varepsilon = \int_{\varepsilon_{th}}^{\infty} \sigma_A(\sigma_0, \varepsilon_0, \varepsilon_{th}, \Gamma; \varepsilon) d\varepsilon, \quad (8)$$

and therefore

$$\mathcal{A} = \sqrt{2\pi} \sigma_0 \Gamma (\varepsilon_0 - \varepsilon_{th}) e^{\Gamma^2/2}. \quad (9)$$

Fitting (3) to the ^4He data we find the four parameters and corresponding 68% C.L. band. The cross section parameters are given in Table I and shown in Fig. 1. For completeness, we also studied the photo-disintegration

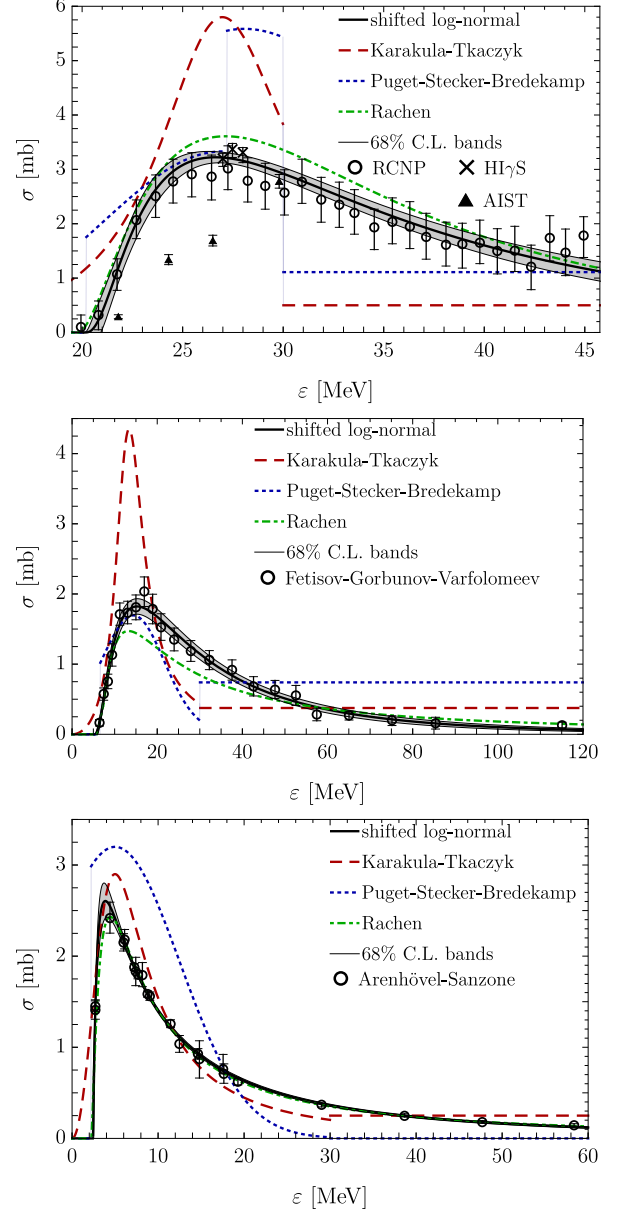


FIG. 1: Best fit and 68% CL bands of the ^4He (top), ^3He (middle), and ^2H (bottom) photo-disintegration cross section. Previous parametrizations of the cross section are also shown for visual comparison; for details one can refer to Appendix A. The experimental data have been taken from [22, 29, 32, 33] (top), [37] (middle), and [38, 39] (bottom).

of secondary ^3He and ^2H . The cross section parameters are also given in Table I and shown in Fig. 1. A comparison of our results with previous approximations (which are briefly summarized in Appendix A) is also exhibited in Fig. 1. The ^3He and ^3H (tritium) have similar photo-disintegration properties. Any possible distinction because of the differences in binding energy due to the Coulomb field disparity would fall within theoretical and experimental uncertainties [39].

To complete our analysis of the photo-disintegration of

TABLE I: Parameters of the photo-disintegration cross-section.

A	σ_0 (mb)	ε_0 (MeV)	ε_{th} (MeV)	Γ	\mathcal{A} (mb MeV)
4	3.22 ± 0.05	26.6 ± 0.4	20.1 ± 0.4	0.94 ± 0.08	77 ± 3
3	1.82 ± 0.05	15.3 ± 0.4	5.1 ± 0.2	0.93 ± 0.04	67 ± 2
2	2.60 ± 0.09	3.87 ± 0.09	2.42 ± 0.05	1.48 ± 0.04	42.2 ± 0.4

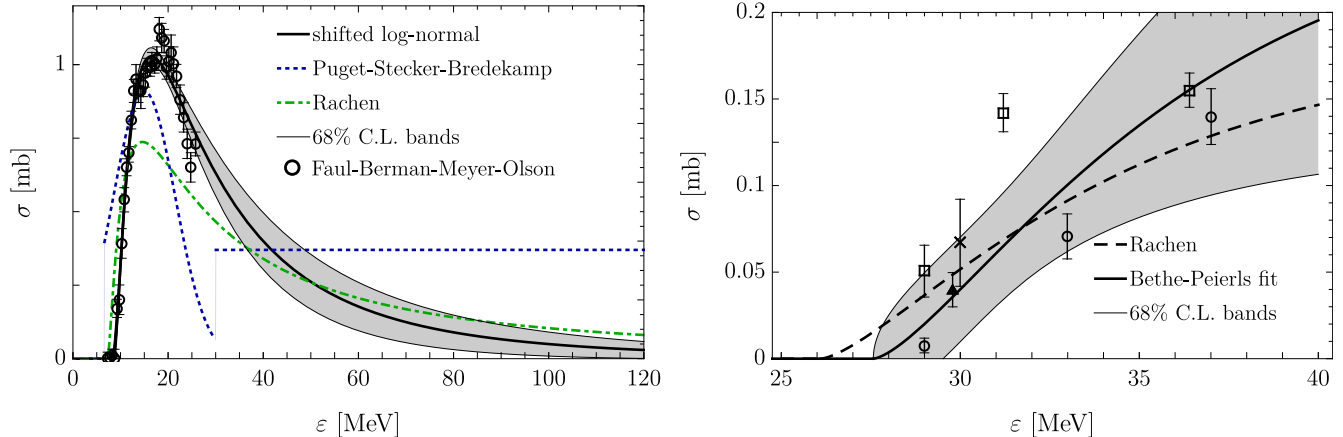


FIG. 2: Best fit and 68% CL bands of the exclusive ${}^3\text{He}(\gamma, pn)\text{H}$ (left) and ${}^4\text{He}(\gamma, pn){}^2\text{H}$ (right) photo-disintegration cross section. Previous parametrizations of the cross section are also shown for visual comparison. The experimental data have been taken from [41, 42] (left) and \blacktriangle [22], \circ [23], \times [16–18], and \square [24] (right).

light nuclei, we provide the relevant branching ratios via fits to the cross-sections for the exclusive three-body processes ${}^3\text{He}(\gamma, pn)\text{H}$ and ${}^4\text{He}(\gamma, pn){}^2\text{H}$. The former can be modeled with a shifted log-normal distribution, the best fit parameters are: $\varepsilon_0 = (16.5 \pm 0.2)$ MeV, $\Gamma = 0.97 \pm 0.07$, $\varepsilon_{th} = (8.1 \pm 0.3)$ MeV, and $\sigma_0 = (1.03 \pm 0.01)$ mb. The latter is best represented by a Bethe-Peierls (BP) form [40],

$$\sigma(\beta, B; \varepsilon) = \beta \times \sigma_{\text{BP}}(B; \varepsilon) = \beta \times \frac{\sigma_{\text{Tp}}}{\alpha_{\text{EM}}} \frac{m_p c^2}{B} \frac{(x-1)^{3/2}}{x^3}, \quad (10)$$

with best fit parameters $\beta = 2.1 \pm 0.5$ and $B = 27.6 \pm 0.7$ MeV. Here, $x = \varepsilon/B$, α_{EM} is the fine structure constant, and σ_{Tp} the Thomson cross section for the proton

$$\sigma_{\text{Tp}} = \frac{8\pi}{3} \left(\frac{\alpha_{\text{EM}} \hbar c}{m_p c^2} \right)^2. \quad (11)$$

In Fig. 2 we show a comparison of the best fit and 68% C.L. bands for the cross sections of three-body processes and previous estimates. To a good approximation, the ratio of the photo-proton ${}^4\text{He}(\gamma, p){}^3\text{H}$ to the photo-neutron ${}^4\text{He}(\gamma, n){}^3\text{He}$ cross sections can be set equal to one [27, 32, 33].

In an aside, it is interesting to note that the Rachen’s parameterization is the closest from all other earlier descriptions to the new experimental data. For instance, Rachen’s description (developed ~ 20 years ago) would produce a higher cross section for ${}^4\text{He}$, what at the end is critical for producing the effect on enlarging the propagation distance that we uncover below, but the general

shape is quite acceptable. Something similar happens for ${}^3\text{He}$ and ${}^2\text{H}$.

III. PHOTO-DISINTEGRATION OF ${}^4\text{He}$ ON THE CMB

We now turn to estimate the GZK energy loss of ultra-relativistic ${}^4\text{He}$ nuclei scattering off the CMB. The relevant mechanisms for the GZK energy loss of UHECR ${}^4\text{He}$ nuclei are: (i) e^+e^- pair production in the field of the nucleus, (ii) photo-disintegration, and (iii) photo-pion production. In the nucleus rest-frame, pair production has a threshold at ~ 1 MeV. The inelasticity of pair production is very low ($\sim m_e/m_p$, for protons), so that the characteristic time-scale of energy loss for this process at energies $E \gtrsim 10^{10}$ GeV is $E/(dE/dt) \approx 10^{9.7}$ yr [43]. For a nucleus, the energy loss rate is Z^2/A times higher than for a proton of the same Lorentz factor [44]. Therefore, for propagation distances $\lesssim 100$ Mpc, pair production from ${}^4\text{He}$ can be safely neglected. For $E \lesssim 10^{11}$ GeV, photo-pion production is also negligible because it has a threshold energy ~ 145 MeV in the nucleus rest frame. In this decade of energy photo-disintegration is the dominant process for energy loss of ${}^4\text{He}$ nuclei: the peak of the GDR corresponds to photon energies of 27 MeV. With this dominance, we now exploit a complete analytic treatment of the GZK energy loss using the simple form of our parametrization.

The interaction time τ_{int} for a highly relativistic nucleus propagating through an isotropic photon back-

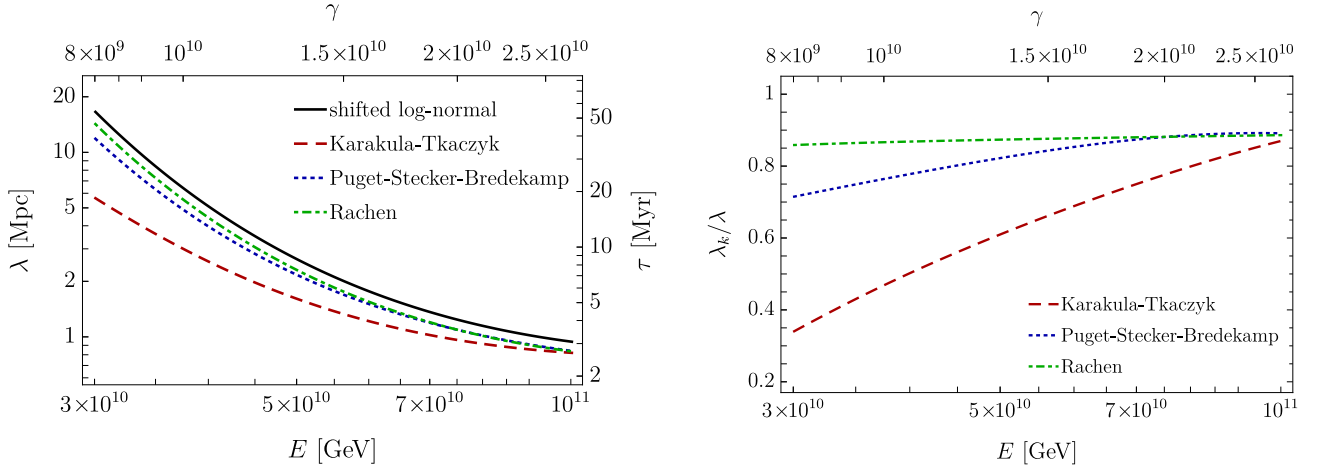


FIG. 3: *Left*: Comparison of the various estimates of the mean free path of UHECR ${}^4\text{He}$ nuclei propagating through the CMB at $z = 0$ (left), and $\lambda_k(\gamma)/\lambda(\gamma)$, for $k \in \{\text{KT, PSB, R}\}$ (right).

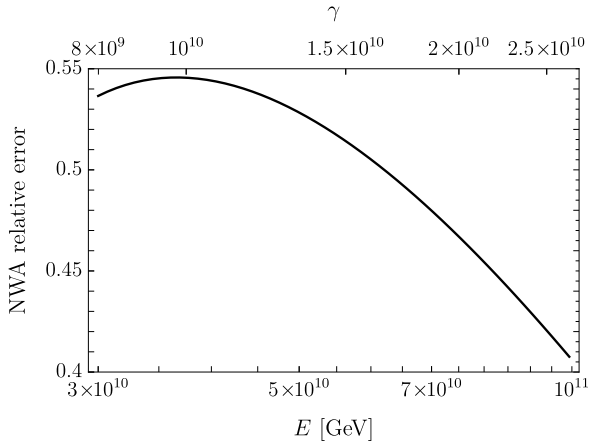


FIG. 4: Relative error $(\lambda - \lambda_{\text{NWA}})/\lambda$ of the NWA.

ground with energy ε and spectrum $dn(\varepsilon)/d\varepsilon$, is [45]

$$\frac{1}{\tau_{\text{int}}} = \frac{c}{2} \int_{\varepsilon_{\text{th}}/2\gamma}^{\infty} \frac{1}{\gamma^2 \varepsilon^2} \frac{dn(\varepsilon)}{d\varepsilon} d\varepsilon \int_{\varepsilon_{\text{th}}}^{2\gamma\varepsilon} \varepsilon' \sigma_A(\varepsilon') d\varepsilon', \quad (12)$$

where $\gamma \sim E/(Am_p)$ is the Lorentz factor and $\sigma_A(\varepsilon')$ is the cross-section for photo-disintegration by a photon of energy ε' in the rest frame of the nucleus. Inserting (7) into (12) we obtain

$$\begin{aligned} \frac{1}{\tau_{\text{int}}} &\approx \frac{c \mathcal{A} \varepsilon_0}{2\gamma^2} \int_{\varepsilon_{\text{th}}/2\gamma}^{\infty} \frac{d\varepsilon}{\varepsilon^2} \frac{dn(\varepsilon)}{d\varepsilon} \Theta(2\gamma\varepsilon - \varepsilon_0) \\ &\approx \frac{\sqrt{\pi} c \sigma_0 \varepsilon_0 (\varepsilon_0 - \varepsilon_{\text{th}}) \Gamma e^{\Gamma^2/2}}{\sqrt{2} \gamma^2} \int_{\varepsilon_0/2\gamma}^{\infty} \frac{d\varepsilon}{\varepsilon^2} \frac{dn(\varepsilon)}{d\varepsilon}. \end{aligned} \quad (13)$$

For the CMB,

$$\frac{dn(\varepsilon)}{d\varepsilon} = \frac{1}{(\hbar c)^3} \left(\frac{\varepsilon}{\pi}\right)^2 [e^{\varepsilon/T} - 1]^{-1}, \quad (14)$$

and so (13) becomes

$$\frac{1}{\tau_{\text{int}}} \approx \frac{\sigma_0 \varepsilon_0 (\varepsilon_0 - \varepsilon_{\text{th}}) \Gamma e^{\Gamma^2/2} T}{\sqrt{2\pi} \pi \hbar^3 c^2 \gamma^2} \left| \ln(1 - e^{-\varepsilon_0/2\gamma T}) \right|, \quad (15)$$

with $T = 2.7255(6)$ K [46].

Despite the computational convenience of the narrow width approximation, a full calculation of the interaction time can be achieved. The second integral in (12) can be calculated exactly for the cross section (3) to give

$$\begin{aligned} J(\varepsilon) &= \int_{\varepsilon_{\text{th}}}^{\varepsilon} \varepsilon' \sigma_A(\varepsilon') d\varepsilon' \\ &= \frac{\mathcal{A}}{2} \left[\varepsilon_{\text{th}} \operatorname{erfc}\left(\frac{\Gamma^2 - z(\varepsilon)}{\sqrt{2}\Gamma}\right) + e^{3\Gamma^2/2} (\varepsilon_0 - \varepsilon_{\text{th}}) \right. \\ &\quad \left. \times \operatorname{erfc}\left(\frac{2\Gamma^2 - z(\varepsilon)}{\sqrt{2}\Gamma}\right) \right]. \end{aligned} \quad (16)$$

For the CMB spectrum, (12) can be rewritten as

$$\frac{1}{\tau_{\text{int}}} = \frac{c}{4\pi^2 (\hbar c \gamma)^3} \int_{\varepsilon_{\text{th}}}^{\infty} \frac{J(\varepsilon)}{e^{\varepsilon/2\gamma T} - 1} d\varepsilon. \quad (17)$$

The integral in (17) is solved numerically, allowing us to obtain the present-day (redshift $z = 0$) mean free path for $A = 4$ nuclei travelling through the CMB with a Lorentz factor γ as

$$\lambda(\gamma) = 4\pi^2 (\hbar c \gamma)^3 \left(\int_{\varepsilon_{\text{th}}}^{\infty} \frac{J(\varepsilon)}{e^{\varepsilon/2\gamma T} - 1} d\varepsilon \right)^{-1}. \quad (18)$$

The mean free path is analogously calculated for the three other models obtaining three functions $\lambda_k(\gamma)$, for $k \in \{\text{KT, PSB, R}\}$, where KT stands for Karakula-Tkaczyk [13], PSB for Puget-Stecker-Bredekamp [12], and R for Rachen [14]; see Appendix A for details. The PSB-model has been the benchmark for the SimProp

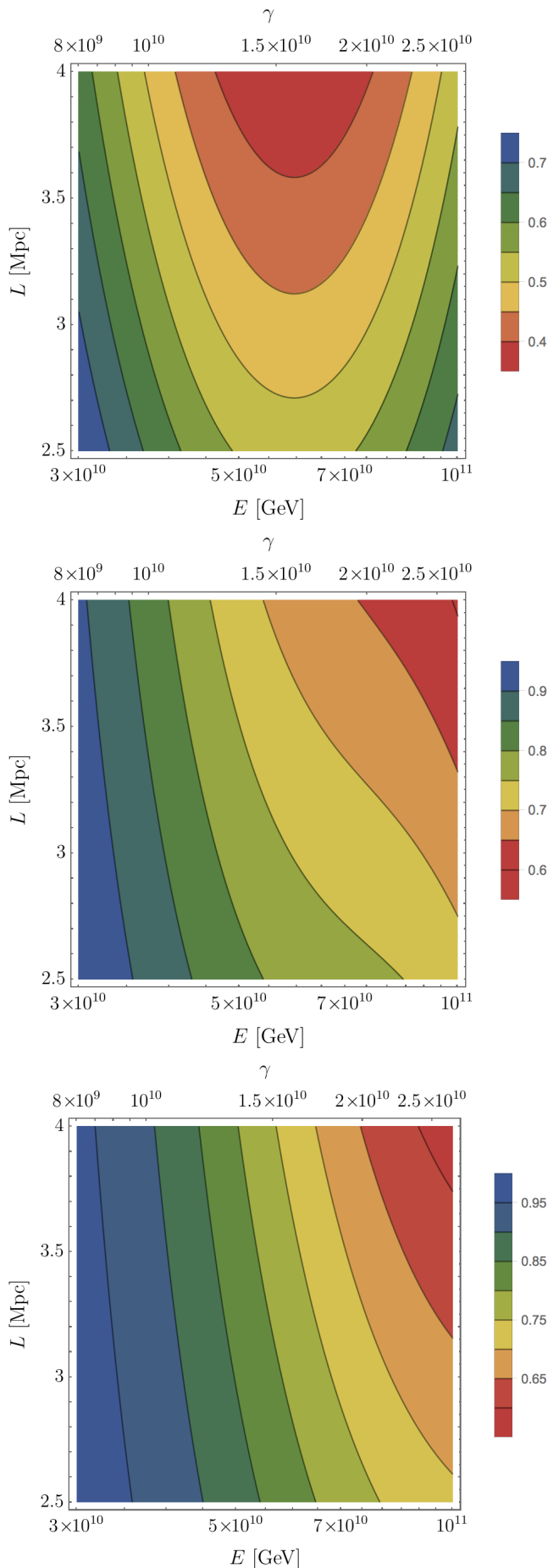


FIG. 5: Relative transmittance for $k = \text{KT}$ (top), $k = \text{PSB}$ medium, and $k = \text{R}$ (bottom).

Monte Carlo code [11] whereas the R-model is used by the CRPropa program [9]. In Fig. 3 we show the mean free path for ${}^4\text{He}$ photo-disintegration on the CMB for the four considered models, and the ratios $\lambda_k(\gamma)/\lambda(\gamma)$ for the three models. In Fig. 4 we display the relative error $(\lambda - \lambda_{\text{NWA}})/\lambda$ of the NWA as a function of energy.

In order to study the consequences that the different cross sections have on particle propagation through the CMB, we study its transmittance to ${}^4\text{He}$ nuclei going through a given distance at a given energy. We define $\mathcal{T}(\gamma, L) \equiv e^{-L/\lambda(\gamma)}$ for the mean free path (18), and $\mathcal{T}_k(\gamma, L) \equiv e^{-L/\lambda_k(\gamma)}$ for the other three models. Since the model introduced in this paper provides the smallest cross section, it will give the largest transmittance. To study this, we define the relative transmittances $R_k(\gamma, L) \equiv \mathcal{T}_k(\gamma, L)/\mathcal{T}(\gamma, L)$. The three ratios are shown in Fig. 5. For a propagation distance of 3.5 Mpc, the transmission of the CMB for our cross-section model at $10^{10.8}$ GeV is $\mathcal{T} \approx 0.11$. Our calculations also demonstrate that if e.g., there was a source a 3.5 Mpc and deflections on the extragalactic magnetic field are small, the Earthly ${}^4\text{He}$ flux would be 35% larger than the output of CRPropa 3 [9] and 42% larger than the output of SimProp v2r4 [11]. For a propagation distance of 4 Mpc, the discrepancy increases as the Earthly fluxes would be 41% and 49% larger than those predicted by CRPropa 3 and SimProp v2r4, respectively. Thus, even for CRPropa 3, which uses the best among the older parameterizations, the differences introduced by a more careful accounting of the ${}^4\text{He}$ photo-disintegration cross section are significant.

For $\gamma \lesssim 10^{9.7}$ the dominant target photons are those of the extragalactic background light. At present, the ambiguity in the determination of infrared (IR) photon background [47–49] largely dominates the uncertainties in the ${}^4\text{He}$ mean-free-path. This is illustrated in Fig. 6 where we show a comparison using the IR estimates from [47] and [49].

IV. CONCLUSION

We have provided new parametrizations for the photo-disintegration cross-section of nuclei with baryon number $A \leq 4$. In our fits we included the most recent cross-section data both from the inclusive measurement observing the analog of the giant dipole resonance in ${}^4\text{He}$ through the charge-exchange spin-flip ${}^4\text{He}({}^7\text{Li}, {}^7\text{Be})$ reaction and from measurements of exclusive two-body and three-body processes: ${}^4\text{He}(\gamma, p){}^3\text{H}$, ${}^4\text{He}(\gamma, n){}^3\text{He}$, and ${}^4\text{He}(\gamma, pn){}^2\text{H}$. A comparison with previous estimates is displayed in Figs. 1 and 2.

We have shown that existing Monte Carlo simulation codes for UHECR propagation underestimate the predicted flux of ${}^4\text{He}$ nuclei emitted by sources in our cosmic backyard. For example, we demonstrated that the mean free path of ${}^4\text{He}$ with $\gamma \sim 10^{10}$ increases by more than 15% with respect to previous estimates adopted as bench-

TABLE II: Parameters for the PSB cross sections.

A	i	$\varepsilon_{\text{th},i}$ (MeV) ^a	$\varepsilon_{0,i}$ (MeV)	Δ_i (MeV)	ξ_i	ζ
4	1	20.2	27	12	0.47	1.11
	2	27.2	45	40	0.11	
3	1	6.6	13	18	0.33	1.11
	2	6.6 ^b	15	13	0.33	
2	1 ^c	2.2	5	15	0.97	—

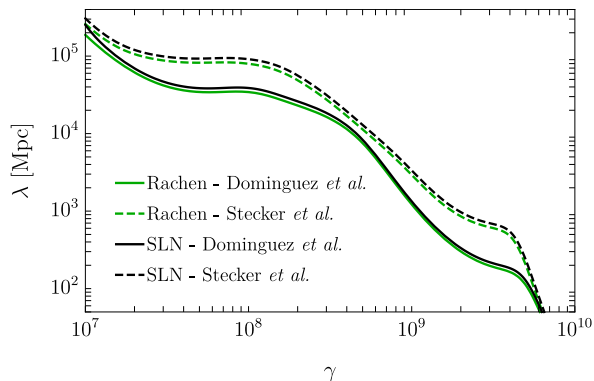


FIG. 6: Photodisintegration mean-free-path of ${}^4\text{He}$ on the IR photon background as estimated in [47] and the lower limit derived in [49]. In the comparison we have used the photodisintegration derived in this work and those obtained earlier by Rachen [14].

marks for Monte Carlo simulation codes of UHECR propagation. A comparison of the different mean-free paths of ${}^4\text{He}$ on the CMB for relevant Lorentz factors is provided in Fig. 3. Interestingly, the larger mean free path obtained in our study implies that the *physical* sur-

vival probability of ${}^4\text{He}$ nuclei would be larger than predicted by existing event generators. For example, for $E \sim 10^{10.8}$ GeV and a propagation distance of 3.5 Mpc, the ${}^4\text{He}$ intensity would be 35% larger than the output of CRPropa 3 program and 42% larger than the output of SimProp v2r4 program. A comparison of the increment in the survival probability of ${}^4\text{He}$ as a function of energy is exhibited in Fig. 5.

As it is obvious, our findings have a direct impact on the possibility that nearby starbursts could relate to the origin of cosmic-rays, what we shall explore elsewhere. It also provides a refreshing humble perspective: basic nuclear physics can still significantly affect our most common assumptions when imagining cosmic ray production sources.

Acknowledgments

This work has been supported by the U.S. National Science Foundation (NSF Grant PHY-1620661), the National Aeronautics and Space Administration (NASA Grant 80NSSC18K0464), as well as by grants AYA2015-71042-P, iLink 2017-1238, and SGR 2017-1383.

Appendix A: Previous parametrizations of the giant dipole resonance

In this Appendix we provide a brief description of the various cross-section models.

Karakula and Tkaczyk (KT) use a Breit-Wigner form to model the peak of the GDR and fit the cross-section to a constant above 30 MeV,

$$\sigma_A^{\text{KT}}(\varepsilon) = \begin{cases} \sigma_0^{\text{KT}} A \frac{(\varepsilon \Gamma)^2}{(\varepsilon^2 - \varepsilon_0^2)^2 + (\varepsilon \Gamma)^2}, & \varepsilon \leq \varepsilon^* \\ A/8 \text{ mb}, & \varepsilon > \varepsilon^* \end{cases}, \quad (\text{A1})$$

with $\Gamma = 8$ MeV, $\varepsilon_0 = 0.925 A^{2.433}$ MeV, $\varepsilon^* = 30$ MeV, and $\sigma_0^{\text{KT}} = 1.45$ mb [13].

Puget, Stecker, and Bredekamp (PSB) also use a piecewise function containing a Gaussian form (2) around the peak of the GDR and a constant above 30 MeV, with normalization given by the TRK dipole sum rule [12, 15]. PSB

^a The source often gives two energy thresholds corresponding to proton and neutron emission [15]. In our calculations we have taken the average value.

^b The source does not provide this energy threshold [15]. Following [42], we assume the energy threshold is similar to that of single nucleon emission.

TABLE III: Parameters for the Rachen cross sections.

A	i	$\beta_{A,i}$	$B_{A,i}$ (MeV)
4	2	1.4	26.1
3	1	1.4	5.8
	2	1.7	7.3
2	1	2.2	1.71

model the total cross section as the sum of (at most) two contributions: single and multiple nucleon emission ($i = 1, 2$ respectively), where

$$\sigma_{A,i}^{\text{PSB}}(\varepsilon) = \begin{cases} \xi_i \Sigma W_i^{-1} \exp\left(-\frac{2(\varepsilon - \varepsilon_{0,i})^2}{\Delta_i^2}\right), & \varepsilon_{\text{th},i} \leq \varepsilon \leq \varepsilon^* \\ \zeta \Sigma / (\varepsilon_{\text{max}} - \varepsilon^*), & \varepsilon^* < \varepsilon \leq \varepsilon_{\text{max}} \\ 0, & \varepsilon > \varepsilon_{\text{max}} \end{cases}, \quad (\text{A2})$$

and where $\varepsilon^* = 30$ MeV, $\varepsilon_{\text{max}} = 150$ MeV, with

$$W_i = \Delta_i \sqrt{\frac{\pi}{8}} \left[\text{erf}\left(\frac{\varepsilon^* - \varepsilon_{0,i}}{\Delta_i / \sqrt{2}}\right) + \text{erf}\left(\frac{\varepsilon_{0,i} - \varepsilon_{\text{th},i}}{\Delta_i / \sqrt{2}}\right) \right]. \quad (\text{A3})$$

The values of ζ , ξ_i , $\varepsilon_{0,i}$ and Δ_i are taken from Table 1 of [12], and the threshold energies $\varepsilon_{\text{th},i}$ are taken from Table 1 of [15]. These values are gathered here and shown in Table II for each A and i .

Rachen (R) uses two functional forms to parametrize the GDR cross-sections of the different nuclei and processes including single ($i = 1$) or multiple ($i = 2$) nucleon emission [14]: (i) the BP form, and (ii) the function

$$\text{Pl}(\varepsilon, \varepsilon_{\text{th}}, \varepsilon_{\text{max}}, \alpha) = \left(\frac{\varepsilon - \varepsilon_{\text{th}}}{\varepsilon_{\text{max}} - \varepsilon_{\text{th}}} \right)^{\alpha(\varepsilon_{\text{max}}/\varepsilon_{\text{th}} - 1)} \left(\frac{\varepsilon_{\text{max}}}{\varepsilon} \right)^{\alpha \varepsilon_{\text{max}}/\varepsilon_{\text{th}}}, \quad \varepsilon > \varepsilon_{\text{th}}, \quad (\text{A4})$$

which has a maximum at ε_{max} and a power law behavior both near threshold and in the asymptotic limit; note that $\text{Pl}(\varepsilon_{\text{th}}, \varepsilon_{\text{th}}, \varepsilon_{\text{max}}, \alpha) = 0$ and $\lim_{\varepsilon \rightarrow \infty} \text{Pl}(\varepsilon, \varepsilon_{\text{th}}, \varepsilon_{\text{max}}, \alpha) \propto \varepsilon^{-\alpha}$.

The cross section for the two-body ${}^4\text{He}(\gamma, p){}^3\text{H}$ and ${}^4\text{He}(\gamma, n){}^3\text{He}$ reactions is described by

$$\sigma_{4,1}^{\text{R}} = 3.8 \text{ mb Pl}(\varepsilon, \varepsilon_{\text{th}}, \varepsilon_{\text{max}}, \alpha), \quad (\text{A5})$$

with $\varepsilon_{\text{th}} = 19.8$ MeV, $\varepsilon_{\text{max}} = 27$ MeV and $\alpha = 5$. The rest of the processes are modelled using the BP form

$$\sigma_{A,i}^{\text{R}} = \beta_{A,i} \sigma_{\text{BP}}(\varepsilon, B_{A,i}), \quad (\text{A6})$$

where the nonzero coefficients are given in Table III.

-
- [1] K. Greisen, **End to the cosmic ray spectrum?**, Phys. Rev. Lett. **16**, 748 (1966). doi:10.1103/PhysRevLett.16.748
- [2] G. T. Zatsepin and V. A. Kuzmin, **Upper limit of the spectrum of cosmic rays**, JETP Lett. **4**, 78 (1966) [Pisma Zh. Eksp. Teor. Fiz. **4**, 114 (1966)].
- [3] D. Allard, N. G. Busca, G. Decerprit, A. V. Olinto and E. Parizot, **Implications of the cosmic ray spectrum for the mass composition at the highest energies**, JCAP **0810**, 033 (2008) doi:10.1088/1475-7516/2008/10/033 [arXiv:0805.4779 [astro-ph]].
- [4] D. Allard, **Extragalactic propagation of ultrahigh energy cosmic-rays**, Astropart. Phys. **39-40**, 33 (2012) doi:10.1016/j.astropartphys.2011.10.011 [arXiv:1111.3290 [astro-ph.HE]].
- [5] L. A. Anchordoqui, V. Barger and T. J. Weiler, **Cosmic mass spectrometer**, JHEAp **17**, 38 (2018) doi:10.1016/j.jheap.2017.12.001 [arXiv:1707.05408 [astro-ph.HE]].
- [6] R. Aloisio, D. Boncioli, A. F. Grillo, S. Petrera and F. Salamida, **SimProp: a simulation code for ultra high energy cosmic ray propagation**, JCAP **1210**, 007 (2012) doi:10.1088/1475-7516/2012/10/007 [arXiv:1204.2970 [astro-ph.HE]].
- [7] K. H. Kampert, J. Kulbartz, L. Maccione, N. Nierstenhoefer, P. Schiffer, G. Sigl and A. R. van Vliet, **CRPropa 2.0: a public framework for propagating high energy nuclei, secondary gamma rays and neutrinos**, Astropart. Phys. **42**, 41 (2013) doi:10.1016/j.astropartphys.2012.12.001 [arXiv:1206.3132 [astro-ph.IM]].
- [8] R. Alves Batista, D. Boncioli, A. di Matteo, A. van Vliet and D. Walz, **Effects of uncertainties in simulations of extragalactic UHECR propagation, using CRPropa and SimProp**, JCAP **1510**, no. 10, 063 (2015) doi:10.1088/1475-7516/2015/10/063 [arXiv:1508.01824 [astro-ph.HE]].

- [9] R. Alves Batista *et al.*, **CRPropa 3: a public astrophysical simulation framework for propagating extraterrestrial ultra-high energy particles**, JCAP **1605**, no. 05, 038 (2016) doi:10.1088/1475-7516/2016/05/038 [arXiv:1603.07142 [astro-ph.IM]].
- [10] D. Boncioli, A. Fedynitch and W. Winter, **Nuclear physics meets the sources of the ultra-high energy cosmic rays**, Sci. Rep. **7**, no. 1, 4882 (2017) doi:10.1038/s41598-017-05120-7 [arXiv:1607.07989 [astro-ph.HE]].
- [11] R. Aloisio, D. Boncioli, A. Di Matteo, A. F. Grillo, S. Petreria and F. Salamida, **SimProp v2r4: Monte Carlo simulation code for UHECR propagation**, JCAP **1711**, no. 11, 009 (2017) doi:10.1088/1475-7516/2017/11/009 [arXiv:1705.03729 [astro-ph.HE]].
- [12] J. L. Puget, F. W. Stecker and J. H. Bredekamp, **Photonuclear interactions of ultrahigh-energy cosmic rays and their astrophysical consequences**, Astrophys. J. **205**, 638 (1976). doi:10.1086/154321
- [13] S. Karakula and W. Tkaczyk, **The formation of the cosmic ray energy spectrum by a photon field**, Astropart. Phys. **1**, 229 (1993). doi:10.1016/0927-6505(93)90023-7
- [14] J. P. Rachen, **Interaction processes and statistical properties of the propagation of cosmic-rays in photon backgrounds**, PhD Thesis, Bohn University (1996).
- [15] F. W. Stecker and M. H. Salamon, **Photodisintegration of ultrahigh-energy cosmic rays: A new determination**, Astrophys. J. **512**, 521 (1999) doi:10.1086/306816 [astro-ph/9808110].
- [16] A. N. Gorbunov and V. M. Spiridonov **Photodisintegration of helium I**, JETP **6**, 16 (1958).
- [17] A. N. Gorbunov and V. M. Spiridonov **Photodisintegration of helium II**, JETP **34 (7)**, 596 (1958).
- [18] A. N. Gorbunov and V. M. Spiridonov **Photodisintegration of helium III**, JETP **34 (7)**, 600 (1958).
- [19] A. N. Gorbunov, V. A. Dubrovina, V. A. Osipova, V. S. Silaeva, and P. A. Cerenkov, **Investigation of the photoeffect in light nuclei**, JETP **15**, 520 (1962).
- [20] A. N. Gorbunov, **Study of the $^4\text{He}(\gamma, p)^3\text{H}$ and $^4\text{He}(\gamma, n)^3\text{He}$ reactions**, Phys. Lett. **27B**, 436 (1968). doi:10.1016/0370-2693(68)90230-X
- [21] E. G. Fuller, H. M. Gerstenberg, H. Vander Molen, and T. C. Dunn, **Photonuclear Reaction Data**, NBS Special Publication 380 (1973).
- [22] T. Shima *et al.*, **Simultaneous measurement of the photodisintegration of He-4 in the giant dipole resonance region**, Phys. Rev. C **72**, 044004 (2005) doi:10.1103/PhysRevC.72.044004 [nucl-ex/0509017].
- [23] Y. M. Arkatov, A. V. Bazaeva, P. I. Vatsset, V. I. Voloshchuk, A. P. Klyucharev and A. F. Khodyachikh, **Three-particle and total photodisintegration of He-4**, Yad. Fiz. **10**, 1123 (1969) [Sov. J. Nucl. Phys. **10**, 639 (1970)].
- [24] F. Balestra, L. Busso, R. Garfagnini, G. Piragino and A. Zanini, **Clustering effects in the photodisintegration of He-4**, Nuovo Cim. A **49**, 575 (1979). doi:10.1007/BF02815786
- [25] B. L. Berman, D. D. Faul, P. Meyer and D. L. Olson, **Photoneutron cross section for He-4**, Phys. Rev. C **22**, 2273 (1980). doi:10.1103/PhysRevC.22.2273
- [26] J. R. Calarco, S. S. Hanna, C. C. Chang, E. M. Diener, E. Kuhlmann and G. A. Fisher, **Absolute cross section for the reaction H-3 (p, gamma0) He-4 and a review of He-4 (gamma, p0) H-3 measurements**, Phys. Rev. C **28**, 483 (1983) Erratum: [Phys. Rev. C **29**, 672 (1984)]. doi:10.1103/PhysRevC.29.672.2, 10.1103/PhysRevC.28.483
- [27] R. Bernabei *et al.*, **Measurement of the He-4(gamma,p)H-3 total cross section and charge symmetry**, Phys. Rev. C **38**, 1990 (1988). doi:10.1103/PhysRevC.38.1990
- [28] B. Nilsson *et al.*, **Near-threshold measurement of the He-4(gamma,n) reaction**, Phys. Lett. B **626**, 65 (2005) doi:10.1016/j.physletb.2005.08.081 [nucl-ex/0506001].
- [29] S. Nakayama *et al.*, **Analog of the giant dipole resonance in He-4**, Phys. Rev. C **76**, 021305 (2007). doi:10.1103/PhysRevC.76.021305
- [30] S. Nakayama *et al.*, **Analogs of the giant dipole and spin-dipole resonances in He-4 and in alpha clusters of Li-6, Li-7 studied by the He-4, Li-6, Li-7 (Li-7, Be-7 gamma) reactions**, Phys. Rev. C **78**, 014303 (2008). doi:10.1103/PhysRevC.78.014303
- [31] T. Shima, Y. Nagai, S. Miyamoto, S. Amano, K. Horikawa, T. Mochizuki, H. Utsunomiya and H. Akimune, **Experimental study of nuclear astrophysics with photon beams**, AIP Conf. Proc. **1235**, 315 (2010). doi:10.1063/1.3442615
- [32] R. Raut, W. Tornow, M. W. Ahmed, A. S. Crowell, J. H. Kelley, G. Rusev, S. C. Stave and A. P. Tonchev, **Photodisintegration cross section of the reaction He-4 (gamma, p) H-3 between 22 and 30 MeV**, Phys. Rev. Lett. **108**, 042502 (2012). doi:10.1103/PhysRevLett.108.042502
- [33] W. Tornow, J. H. Kelley, R. Raut, G. Rusev, A. P. Tonchev, M. W. Ahmed, A. S. Crowell and S. C. Stave, **Photodisintegration cross section of the reaction He-4 (gamma, n) He-3 at the giant dipole resonance peak**, Phys. Rev. C **85**, 061001 (2012). doi:10.1103/PhysRevC.85.061001
- [34] W. Thomas, **Über die Zahl der Dispersionselektronen, die einem stationren Zustande zugeordnet sind** Die Naturwissenschaften **13**, 627 (1925) doi:10.1007/BF01558908.
- [35] F. Reiche and W. Thomas, **Über die Zahl der Dispersionselektronen, die einem stationren Zustand zugeordnet sind** Z. Phys. **34**, 510 (1925).
- [36] W. Kuhn, **Über die Gesamtstärke der von einem Zustande ausgehenden Absorptionslinien** Z. Phys. **33**, 408 (1925).
- [37] V. N. Fetisov, A. N. Gorbunov, and A. T. Varfolomeev, **Nuclear photoeffect on three-particle nuclei**, Nucl. Phys. **71**, 305 (1965)
- [38] H. Arenhovel and M. Sanzone, **Photodisintegration of the deuteron: A review of theory and experiment**, Few Body Syst. Suppl. **3**, 1 (1991).
- [39] S. Bacca and S. Pastore, **Electromagnetic reactions on light nuclei**, J. Phys. G **41**, no. 12, 123002 (2014) doi:10.1088/0954-3899/41/12/123002 [arXiv:1407.3490 [nucl-th]].
- [40] H. Bethe and R. Peierls **Quantum theory of the diplon**, Proc. Roy. Soc. A **148**, 146 (1935).
- [41] D. D. Faul, B. L. Berman, P. Meyer and D. L. Olson, **Photodisintegration of H-3 and He-3**, Phys. Rev. C **24**, 849 (1981). doi:10.1103/PhysRevC.24.849
- [42] R. Skibinski, J. Golak, H. Witala, W. Gloeckle, H. Kamada and A. Nogga, **Three nucleon photodisintegration of He-3**, Phys.

- Rev. C **67**, 054002 (2003) doi:10.1103/PhysRevC.67.054002 [nucl-th/0301051].
- [43] F. A. Aharonian and J. W. Cronin, **Influence of the universal microwave background radiation on the extragalactic cosmic ray spectrum**, Phys. Rev. D **50**, 1892 (1994). doi:10.1103/PhysRevD.50.1892
- [44] M. J. Chodorowski, A. A. Zdziarski, and M. Sikora, **Reaction rate and energy-loss rate for photopair production by relativistic nuclei**, Astrophys. J. **400**, 181 (1992). doi: 10.1086/171984
- [45] F. W. Stecker, **Photodisintegration of ultrahigh-energy cosmic rays by the universal radiation field**, Phys. Rev. **180**, 1264 (1969). doi:10.1103/PhysRev.180.1264
- [46] D. J. Fixsen, **The temperature of the cosmic microwave background**, Astrophys. J. **707**, 916 (2009) doi:10.1088/0004-637X/707/2/916 [arXiv:0911.1955 [astro-ph.CO]].
- [47] A. Dominguez *et al.*, **Extragalactic background light inferred from AEGIS Galaxy SED-type fractions**, Mon. Not. Roy. Astron. Soc. **410**, 2556 (2011) doi:10.1111/j.1365-2966.2010.17631.x [arXiv:1007.1459 [astro-ph.CO]].
- [48] R. C. Gilmore, R. S. Somerville, J. R. Primack and A. Dominguez, **Semi-analytic modeling of the EBL and consequences for extragalactic gamma-ray spectra**, Mon. Not. Roy. Astron. Soc. **422**, 3189 (2012) doi:10.1111/j.1365-2966.2012.20841.x [arXiv:1104.0671 [astro-ph.CO]].
- [49] F. W. Stecker, S. T. Scully and M. A. Malkan, **An empirical determination of the intergalactic background light from UV to FIR wavelengths using FIR deep galaxy surveys and the gamma-ray opacity of the Universe**, Astrophys. J. **827**, no. 1, 6 (2016) doi:10.3847/0004-637X/827/1/6 [arXiv:1605.01382 [astro-ph.HE]].